

Nanocrystalline material development for high-power inductors

Jianguo Long and Mike McHenry

Department of Material Science and Engineering, Carnegie Mellon University, Pittsburgh, Pennsylvania 15213, USA

Damian P. Urciuoli^{a)}

Sensors and Electron Devices Directorate, U.S. Army Research Laboratory, Adelphi, Maryland 20783, USA

Vladimir Keylin and Joe Huth

Magnetics Technology Center, Division of Spang & Co., Pittsburgh, Pennsylvania 15213, USA

Thomas E. Salem

Department of Electrical Engineering, U.S. Naval Academy, Annapolis, Maryland 21402, USA

(Presented on 6 November 2007; received 6 September 2007; accepted 1 October 2007; published online 22 January 2008)

A new high-saturation induction, high-temperature nanocomposite alloy for high-power inductors is discussed. This material has FeCo with an A2 or B2 structure embedded in an amorphous matrix. An alloy of composition $\text{Fe}_{56}\text{Co}_{24}\text{Nb}_4\text{B}_{13}\text{Si}_2\text{Cu}_1$ was cast into a 1.10 in. wide, 0.001 in. thick ribbon from which a toroidal core of approximately 4.25 in. outer diameter, 1.38 in. inner diameter, and 1.10 in. tall was wound. The core was given a 2 T transverse magnetic field anneal, and impregnated for strength. Field annealing resulted in a linear B - H response with a relative permeability of 1400 that remained constant up to field strengths of 1.2 T. The core was used to construct a 25 μH inductor for a 25 kW dc-dc converter. The inductor was rated for operation in discontinuous conduction mode at a peak current of 300 A and a switching frequency of up to 20 kHz. Compared to commercially available materials, this new alloy can operate at higher flux densities and higher temperatures, thus reducing the overall size of the inductor. © 2008 American Institute of Physics. [DOI: 10.1063/1.2829033]

INTRODUCTION

Electrical conversion systems have become smaller and lighter predominantly from advancements in active components, which have allowed increased converter switching frequencies. This has enabled size and weight reductions of the passive components of these systems. As a result, compact multikilowatt power converters are finding applications on many platforms, such as hybrid electric vehicles, where space and weight are constrained.¹ Still, magnetic components occupy a large portion of these converters. By reducing the size of these magnetic components through advancements in magnetic material composition and processing, significant benefits at the power converter system level can be realized.

Nanocomposite magnetic materials can offer a combination of properties which facilitate component size reduction. These alloys are comprised of ultrafine nanocrystalline grains homogeneously dispersed in an amorphous matrix. The excellent soft magnetic properties of these materials, such as low coercivities, high permeabilities, and low energy losses, have triggered major interest in both fundamental and applied researches. Applications have been identified using the patented FeSiNbBCu and FeMBCu alloys.^{2,3} Other nanocrystalline soft magnetic alloys based on the FeCo system called HITPERM have been reported for high-temperature application.^{4,5}

A new class of FeCo based experimental nanocrystalline alloys (HTX) that exhibits high-saturation induction, high-temperature stability, and low loss has recently been developed.^{6,7} From this family of materials, the HTX 002 alloy was selected for use in an inductor for a future hybrid ground vehicle 25 kW dc-dc prototype converter. This paper presents the composition of the nanocomposite alloy, the material processing of the power inductor core, and the fabrication of the inductor along with its performance in a converter operated up to 25 kW.

MATERIAL DEVELOPMENT

A nanocomposite soft magnetic alloy ($\text{Fe}_{56}\text{Co}_{24}\text{Nb}_4\text{B}_{13}\text{Si}_2\text{Cu}_1$) was cast into ingots and analyzed by inductively-coupled plasma spectrometry to confirm that the target chemistry was achieved. The Fe:Co ratio was maintained at 0.7:0.3 to obtain high-saturation induction. Nb played an important role in impeding the growth of nanocrystals and facilitated casting in air, as compared to Zr glass formers. The ingots were then processed using planar flow casting (PFC) equipment for remelting and ribbon production. PFC allows direct casting of a continuous ribbon of uniform thickness and is the only commercially viable method of producing most amorphous and nanocrystalline alloys, since the ribbon must be cooled quickly enough to prevent crystallization. The PFC consists of a bottom-casting crucible, casting nozzle, stopper rod, an *in situ* thermocouple, a variable-speed water-cooled copper alloy casting

^{a)}Electronic mail: durciuoli@arl.army.mil.

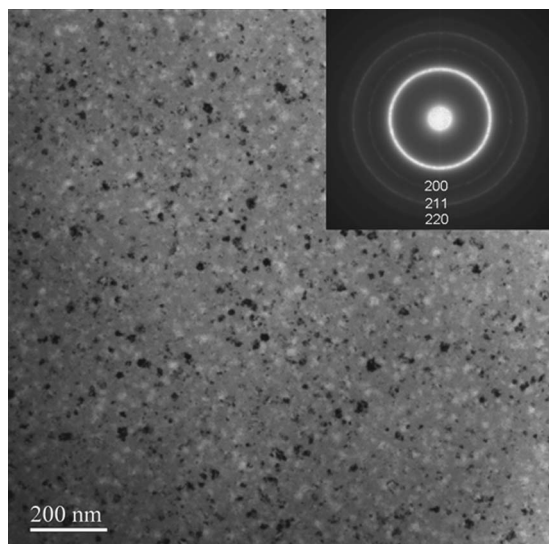


FIG. 1. TEM bright field view image of the sample annealed at 450 °C for 1 h.

wheel, and an induction coil with a high-frequency power supply. The caster operation required precise control of several operating parameters to achieve a narrow processing window that resulted in good quality ribbon.

The x-ray diffraction (XRD) pattern of the cast ribbon in its nanocrystalline state after annealing amorphous precursor at 450 °C for 1 h showed broad diffraction peaks indicating that the ribbon was amorphous and the primary crystallization product was a bcc FeCo lattice structure with an average grain size of 12 nm. Figure 1 shows the transmission electron microscopy (TEM) bright field image of a sample annealed at 450 °C. The differential thermal analysis (DTA) curve for a 5 °C/min heating rate shows three crystallization peaks. Primary crystallization began at 420 °C with a maximum at 442 °C. The secondary and tertiary crystallization peaks were at 672 and 766 °C, respectively.

After XRD analysis, the thickness, surface smoothness, and ductility of the ribbon were evaluated and tape cores were wound to the desired dimensions. Each core was impregnated with an inorganic binder prior to annealing to impart strength. In an inert atmosphere at varying temperatures, a transverse-magnetic field, as high as 2.0 T, was used to anneal the core. The heat rate was carefully controlled to avoid self-heating during the exothermic crystallization reaction. This annealing profile resulted in a linear B - H response and a constant permeability of 1400 up to a field strength of 1.2 T.

The cores treated with a transverse magnetic field applied throughout the annealing cycle had lower losses and lower remanence ratios, compared to cores annealed under a magnetic field during the cooling portion of the cycle. These properties, in addition to saturation induction which was measured at a maximum of 1.47 T, were seen to be thermally stable up to 300 °C. Figures 2 and 3 show power loss versus flux density at selected frequencies and maximum saturation flux density versus temperature, respectively. Losses were measured to be 3.8 W/kg at 0.2 T and 20 kHz; and 1.5 W/kg at 0.02 T and 200 kHz as compared to

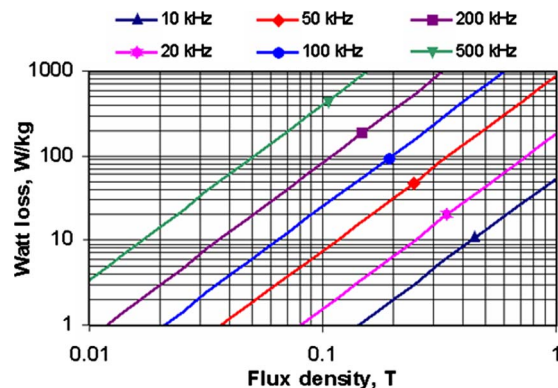


FIG. 2. (Color online) Watt loss vs flux density at select frequencies.

1.9 W/kg and 1.2 W/kg, respectively, for commercially available FINEMET FT-3 nanocrystalline material. The HTX 002 material also exhibited a saturation magnetostriction of 21 ppm, which indicated a relatively high sensitivity to mechanical stress. As a result, impregnating and cutting the cores to allow gapping can increase losses by up to a factor of 3.

INDUCTOR CONSTRUCTION AND PERFORMANCE

The inductor configuration was based on a previous design that incorporated an eight turn copper winding insulated with Nomex® around the toroid.⁸ An aluminum base plate was fabricated to mate to the bottom surface of the core and served as a heat spreader to a commercially available liquid cold plate. The core was bonded to the base plate by a thermally conductive electrically insulating epoxy, and thermal compound was used at the interface between the base plate and cold plate. The inductance of this configuration was measured to be 24.2 μ H at 10 kHz.

A 25 kW dc-dc converter power stage was used to evaluate the inductor. The power stage was operated at a switching frequency of 15 kHz. To ensure that the inductor current was always in the discontinuous conduction mode, duty cycles of 40%–45% were run to attain each power level at its corresponding voltage setting. The inductor was actively cooled by its attached liquid cold plate using a 50% by volume aqueous solution of propylene glycol at 23 °C and a flow rate of 1.1 gpm (gpm denote gallons per minute). A thermal map of the average core and winding temperatures at each operating power level was obtained using an infrared camera.⁹ The maximum core temperature of 80 °C occurred at the 25 kW operating point which corresponded to a peak inductor current of 282 A. This result was an increase of

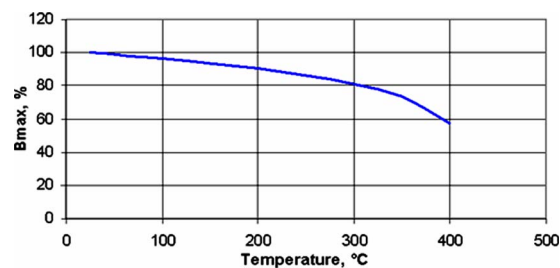


FIG. 3. (Color online) Maximum saturation flux density thermal stability.

15.5% in average core temperature compared to results obtained from a similarly constructed inductor using FINEMET® FT-3 core material. Yet the HTX 002 based inductor had a 39% reduction in core volume with identical electrical performance.

CONCLUSIONS

A new high-saturation induction, high-temperature nanocrystalline alloy of composition $\text{Fe}_{56}\text{Co}_{24}\text{Nb}_4\text{B}_{13}\text{Si}_2\text{Cu}_1$ for high-power inductors has been developed. The core wound from this alloy was impregnated for strength and given a 2 T transverse magnetic field anneal which produced a linear B - H response with a relative permeability of 1400 that remained constant up to field strengths of 1.2 T. From this core, a 25 μH inductor was constructed for use in a 25 kW dc-dc converter. The inductor was rated for operation at a peak current of 300 A and a switching frequency of up to 20 kHz. Compared to commercially available materials, the HTX 002 alloy can operate at higher flux densities, higher temperatures, and reduces the overall size of the inductor.

ACKNOWLEDGMENTS

This work was supported by the National Science Foundation (DMR-0406220) and the U.S. Army Research Labo-

ratory (under cooperative agreement W911NF-04-2-0017). The views and conclusions contained in this document are those of the authors and should not be interpreted as representing the official policies, either expressed or implied, of the U.S. Army Research Laboratory or the U.S. Government. The U.S. Government is authorized to reproduce and distribute reprints for Government purposes notwithstanding any copyright notation hereon.

¹D. Urciuoli and C. W. Tipton, Proceedings of the IEEE APEC (IEEE, Dallas, TX, 2006), pp. 1375–1378.

²Y. Yoshizawa, S. Oguma, and K. Yamauchi, J. Appl. Phys. **64**, 6044 (1988).

³K. Suzuki, N. Ktaoka, A. Inoue, A. Makino, and T. Masumoto, Mater. Trans., JIM **31**, 743 (1990).

⁴M. A. Willard, D. E. Laughlin, M. E. McHenry, D. T. K. Sickafus, J. O. Cross, and V. G. Harris, J. Appl. Phys. **84**, 6773 (1998).

⁵M. E. McHenry, M. A. Willard, and D. E. Laughlin, Prog. Mater. Sci. **44**, 291 (1999).

⁶J. Long, Y. Qin, T. Nuhfer, M. De Graef, D. E. Laughlin, and M. E. McHenry, J. Appl. Phys. **101**, 09N115 (2007).

⁷J. Long, P. R. Ohodnicki, D. E. Laughlin, and M. E. McHenry, J. Appl. Phys. **101**, 09N114 (2007).

⁸T. E. Salem, D. P. Urciuoli, V. Lubomirsky, and G. K. Ovrebø, Proceedings of the IEEE APEC, (IEEE, Anaheim, CA, 2007), pp. 1258–1263.

⁹T. E. Salem, D. Ibitayo, and B. R. Geil, Proceedings of the IEEE Inst. Meas. Tech. Conf., (IEEE, Ottawa, Ontario, Canada, 2005), pp. 829–833.